33rd Annual International Conference of the IEEE EMBS
Boston, Massachusetts USA, August 30 - September 3, 2011

Planar Saline Bath Phantom of the Rush Head Model

Clarissa Shephard, Thomas Jochum, *IEEE Member*, Zachary Abzug, and Patrick Wolf

Abstract— **The Rush head model is an approximation of the volume conducting properties of the human head. A planar saline bath phantom was developed to simulate the key properties of the Rush head model while creating a testing platform for implantable neural devices. The phantom closely mimics electrical properties of human tissue such as increased resistivity through the skull region and current flow that wraps around the head. Preliminary testing shows good agreement of the saline bath phantom to predictions from a computer model.**

I. INTRODUCTION

RUSH developed the three-sphere model of the human head as a simplified representation of the true head anatomy [1]. The homogeneous layers in the model represent the brain, skull, and scalp with radii of 8.0, 8.5, and 9.2 cm respectively and a brain:skull:scalp resistivity ratio of 1:25:1 (Fig. 1a). The Rush model is a cornerstone in neural electrophysiological research and appears in hundreds of citations. Physical realizations of head models, such as a resistor mesh model [2] and a gelatin model [3] have been constructed; however, these are not practical when conducting multiple experiments involving implanted devices of different sizes, depths, and locations within the scalp. A saline bath is a more convenient analog of tissue [4], but a spherical saline bath presents obvious difficulties. A planar saline bath phantom was developed to create a simple testing platform for cranial implant experimentation while maintaining the major properties of the Rush head model, including the ability for current between two electrodes on the scalp to wrap around the scalp in all directions as well as pass through the high resistance of the skull and into the brain.

II. METHODS

A. Phantom Construction

Each concentric region of the Rush head model was projected onto a thin planar region according to the HEALPix discontinuous conformal mapping technique (Fig. 1b) [5, 6, 7]. Many planar projections of a spherical surface have been developed. None of these projections maintain surface distances. However, the HEALPix model maintains surface area. Preservation of surface area is useful for modeling surface-area dependent effects such as absorbing electromagnetic energy or emitting heat via convection.

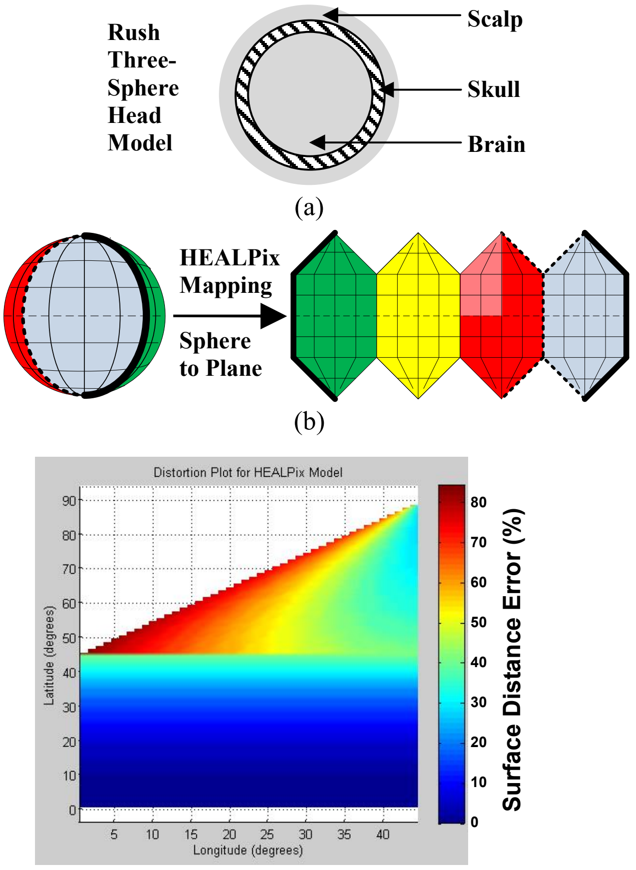

(a)

(b)

(c)

Figure 1: (a) The Rush head model is a spherical core for the brain and outer layers for the skull and scalp. (b) The HEALPix projection maps the surface of a sphere onto a plane. (c) The HEALPix projection distorts surface distances along the 0°, 90°, 180° and 270° longitudes. Only the light red region in Fig. 1b is plotted in Fig. 1c.

The HEALPix projection maintains accurate surface distances only along the equator, allowing for accurate measurements of distance-dependent effects such as the electric field and current flow there (Fig 1c). The HEALPix projection has severe distortion where the lines of longitude bend, limiting the usefulness of the model if the phenomenon being studied is critically dependent on these regions.

An acrylic assembly, based on the HEALPix projection, is placed in a saline bath to mimic the electrical properties of biological tissue (Fig. 2). To achieve the desired dimensions and resistivity, the brain and scalp are modeled as 7 and 80 mm thick layers of saline with a resistivity of 3 ohm*meter

---

Manuscript received April 15, 2011; revised June 19, 2011. C. Shephard was supported by National Science Foundation Research Experiences for Undergraduates Grant No. 0754963 administered by The Pratt School of Engineering at Duke University.

C. Shephard was with North Carolina State University, Raleigh, NC 27695 USA (email: cjshepha@ncsu.edu). She will attend the Georgia Institute of Technology.

T. Jochum, Z. Abzug, and P. Wolf (corresponding author) are with Duke University, Durham, NC 27708 USA (email: thomas.jochum@duke.edu, zachary.abzug@duke.edu, patrick.wolf@duke.edu, phone: 919-660-5114).

978-1-4244-4122-8/11/$26.00 ©2011 IEEE

(0.3M NaCl) [8]. The increased resistivity of the skull is modeled by a 5 mm thick acrylic sheet (Chemcast GP) perforated with 1 mm radius holes on a 9 mm x 9 mm grid to create a 4% open area material.

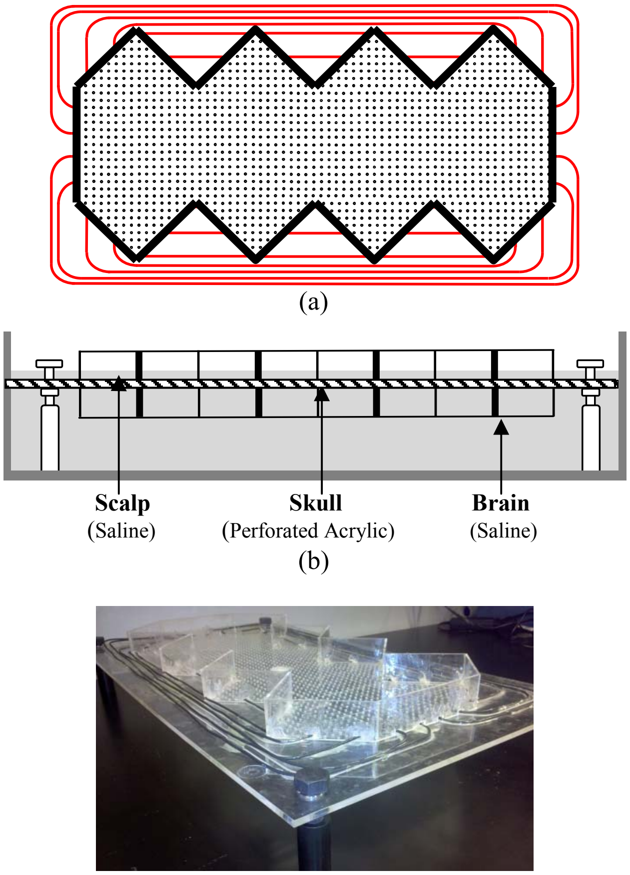
(a)

(b)

(c)

Fig. 2: (a) Aerial view of the acrylic assembly. The walled interior region is 58 by 29 cm. (b) Cross-sectional view of the saline bath phantom. (c) Photo of the acrylic assembly.

As portrayed in Fig. 2a, the thick black lines represent the trenches cut into the acrylic sheet to position the acrylic side walls that restrict current flow to within the scalp and skull. The red lines are 14 gauge copper wires used to electrically connect regions of the scalp that would be connected in the three-sphere model, but are physically disconnected in the projection. The ends of the wires are inserted just inside the walls with approximately 2 mm of insulation removed. Similar wires connect the upper layer of the brain.

In Fig. 2b, the acrylic walls (37 mm tall, 3 mm thick) used to restrict the current flow within the scalp and brain regions can be seen above and below the crosshatched region that represents the perforated acrylic skull. All acrylic pieces were machined with a Universal Laser System VLS 6.60. (Machining files are available.) Plastic bolts and spacers were used to suspend the assembly in saline. The assembly sagged a few mm in the middle so horizontal supports (not shown) were attached.

B. Phantom Measurements

To verify the use of perforated acrylic as a means to increase the resistance, a test piece was created with perforations identical to the full model (Fig. 3). A lateral voltage was created in the saline by driving the working electrodes with an AC voltage source. The amplitude of the source was adjusted to maintain constant amplitude on the sense electrodes. Voltage measurements were made (Keithley 2000 Multimeter) across the perforated piece and across the saline. The ratio of the potential drop across the skull to the potential drop across the saline was used as a representation of the skull:scalp resistivity ratio for comparison to the desired ratio of 25:1.

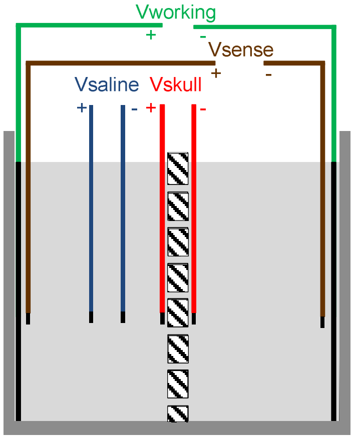

Fig. 3: Experimental set-up to test resistivity of perforated acrylic as a skull substitute.

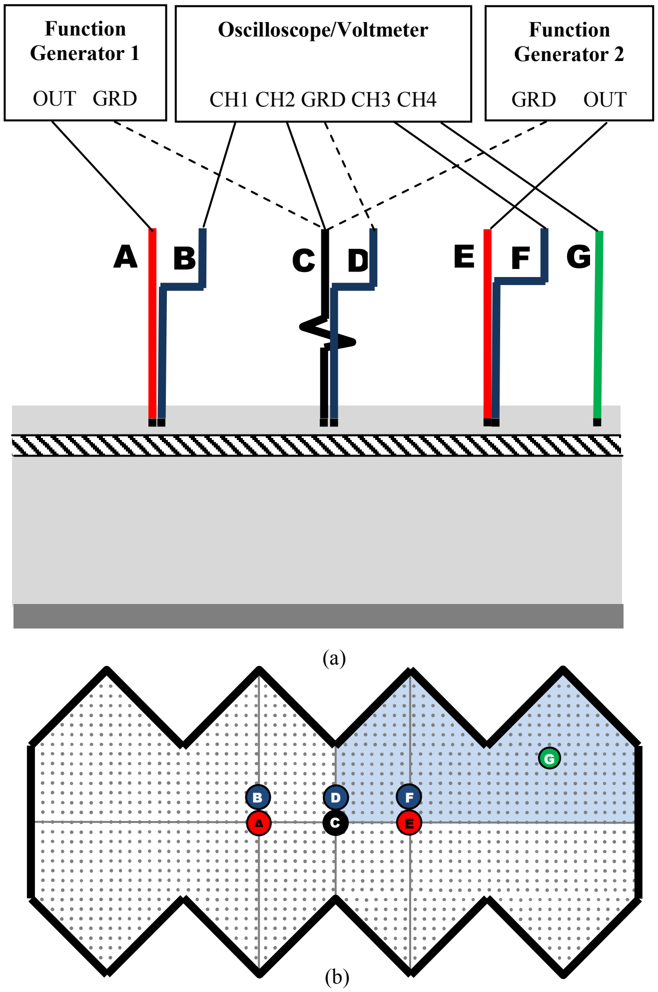

(a)

(b)

Fig. 4: Experimental set-up to test the electrical properties of the saline phantom. (a) Cross-sectional view of the measurement system. (b) Aerial view of the probe locations.

Fig. 4 shows the experimental set-up used to measure voltages and resistances in the phantom. The set-up used two Agilent 33220A function generators, applied at electrodes A and E, with equal-amplitude 100 kHz sine waves of opposite polarity to create a neutral voltage line along the center and lateral edges of the model. The location of electrodes A and E matches the location of the electrodes of an experimental implanted device. To ensure that the function generators had equal current amplitudes, the amplitude of one was adjusted until the voltage at node C was zero. A frequency of 100 kHz was chosen for the low impedance at the saline-probe interface and the high input impedance of the test equipment relative to the saline. The model symmetry allowed for measurements to be taken in only one-quarter of the saline-bath (shaded region of Fig. 4b). The mobile electrode, G, was used to measure the potential with a Keithley 2000 Multimeter and Tektronix TDS 340A Oscilloscope. The voltages measured on electrode G were scaled by the voltage on F so that variation in the saline resistivity or probes A and E impedance did not influence the data.

Three measurements were performed with the test set-up shown in Fig. 4:

(1) The potential was measured at every perforation (gray dots in Fig. 4b) to determine the similarity between the volume conducting properties of the phantom and those of a computer simulation (COMSOL) of both the true three-sphere model and a simulation of the actual saline bath phantom.

(2) The copper wires create a low impedance electrical connection between physically disconnected regions of the model. Measurements were taken with and without the wires to determine the effect of the wires on model connectivity. To block the conductance of the wires, petroleum jelly was used to cover the exposed copper wire tips. The effect-of-wires measurements were compared to the equivalent computational model.

(3) To quantify the division of current between the scalp and the brain, the relative resistance between electrodes B and F was found when the brain and skull regions were blocked versus unblocked. The skull and brain were blocked by covering the perforations with 0.25 mm thick Mylar.

III. RESULTS

Table 1 gives the ratio of the potential across the perforated acrylic to the potential through the saline (see Fig. 3 for set-up). The results closely resemble the desired 25:1 ratio.

TABLE I
RESULTS OF SKULL RESISTANCE MEASUREMENTS

Frequency	Ratio
10 kHz	27.5
100 kHz	27.7
1 MHz	27.6

The results of the three measurements on the saline-bath phantom (Fig. 4) are:

(1) The predicted voltages from COMSOL for the three dimensional Rush head model were plotted on a HEALPix grid (Fig. 5a) for easier comparison to the saline bath models. The measured voltages for the phantom (Fig. 5c) were compared to the predicted voltages from COMSOL (Fig. 5b). The maximum error was 3% of full scale (Fig. 5d).

(2) Measurements were made in the phantom and calculated in the COMSOL model with the wires connected and disconnected (Fig. 6). With the wires connected, the voltage in the phantom decayed to nearly zero at 180 degrees as predicted by COMSOL. With the wires disconnected, the voltage in the phantom also decayed at higher longitudes unlike the COMSOL prediction.

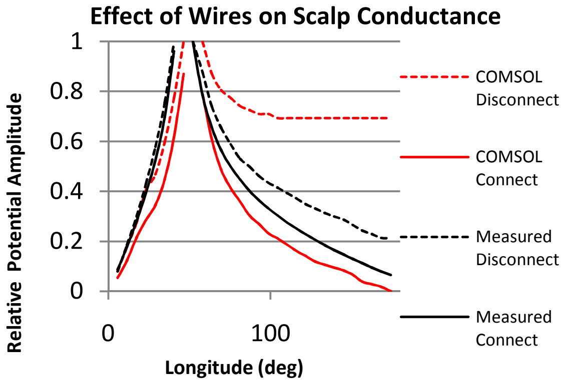

Figure 6: Effect of the copper wires on the scalp potential as measured in the saline-bath phantom (black) and estimated in the computational model (red). All measurements were taken at zero latitude.

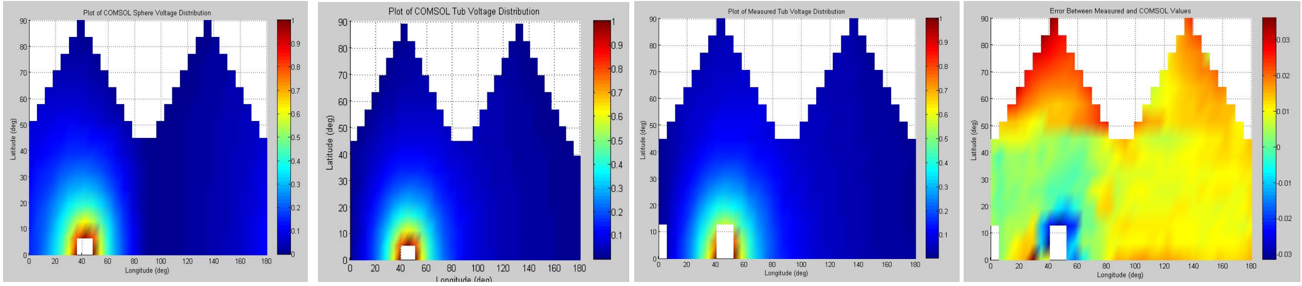

(a) (b) (c) (d)

Figure 5: (a) Relative voltages from the COMSOL three-sphere model mapped onto the HEALPix projection. (b) COMSOL prediction for the phantom. (c) Measured values from the phantom. (d) Error between measured values (Fig. 5c) and COMSOL phantom model (Fig. 5b). The maximum errors of 3% are near the poles and the electrodes. In all four plots, blank squares correlate to locations where electrodes A through F prevented measurements.

(3) The ratio was calculated for the resistance of the entire model (scalp, skull, and brain) to the resistance of the scalp alone. This comparison was made for the phantom, the COMSOL model of the phantom, and the COMSOL model of the Rush three-sphere model. The data (Table 2) shows the discrepancy between the COMSOL calculations and the measured data. (The raw measured data is 682 ohms for the scalp alone and 306 ohms with the skull and scalp.)

TABLE 2
RELATIVE RESISTANCE OF SCALP WITH VERSUS WITHOUT THE SKULL AND BRAIN

Scenario	Ratio
COMSOL Sphere	0.63
COMSOL Planar Bath	0.57
Measured	0.45

IV. DISCUSSION

The saline bath error plot (Fig. 5d) and the effect-of-wires measurements (Fig. 6) support the key goal for a phantom of the Rush model, namely, current flow in all directions. However, the effect-of-wires measurements (Fig. 6 solid black curve) do not reach zero at 180 degrees. This may be due to wire inductance of ~1 μH and the copper-saline interface impedance [9, 10]. The COMSOL model predicts a constant potential in the 90-180 degree longitude region when the wires are removed (Fig. 6 dotted red curve). However, the measured values did not have a constant potential in the outer regions of the model (Fig. 6 dotted black curve). The decay in the measured voltage may be caused by current flow due to the capacitive properties of the Mylar used to block the skull perforations, the impedance of probe G, or magnetic coupling of the scalp saline to the brain saline.

Significant differences were seen between the relative resistance ratio of the scalp with and without the skull and brain regions (Table 2). This discrepancy uncovered a necessary improvement to the phantom; the depth of the brain region should be 5 cm instead of 8 cm. The 8 cm depth was chosen to match the radius of the Rush model but COMSOL modeling of the phantom revealed that a 5cm depth would give the correct effect of skull and brain on the total resistance. Another possible cause for the low measured value in Table 2 is that COMSOL did not include magnetic coupling between saline and wires in the scalp to saline and wires in the brain. This causes an overestimation of effective resistance of the brain region in COMSOL.

The results in Table 1 demonstrate that properly dimensioned holes in an acrylic sheet can create a desired skull resistivity. The skull resistivity selected for this model is smaller than in the Rush model which had a 1:80:1 ratio of scalp:skull:brain. Rush based the skull resistivity on *in vitro* measurements. More recent *in vivo* measurements found ratios of 1:15:1 [11] to 1:42:1 [12]. The model presented here has a compromise value of 1:28:1.

V. CONCLUSION

A planar saline bath phantom of the Rush three-sphere head model was created using the HEALPix projection. Key technical goals of the Rush model, including the ability of current to flow in all directions around the head and pass through the high resistance skull into the brain, were met. Given the importance of stray reactive impedance effects associated with the wire connections and the difference in the frequency dependent impedance of saline and tissue[8], care should be taken using this model at frequencies above 100 kHz.

The techniques developed here can be applied to building a more sophisticated planar phantom of realistic head geometry or of other approximately spherical organs, such as the heart or eye. The phantom will be used to measure the efficiency and heat absorption of an experimental technique of transferring power transcutaneously to an implanted electronic device. The phantom may also be used to verify the many applications that have been modeled with the Rush three-sphere head model. These applications include EEG source locating, telemetry to or from an implanted device, and surface or deep neural stimulation.

ACKNOWLEDGMENT

The authors thank Matt Brown, Steve Earp, and Marcus Henderson for construction advice, material, and equipment, Ned Danieley for computer support, and the anonymous reviewers for their corrections and suggestions.

REFERENCES

[1] S. Rush, "Current distribution in brain from surface electrodes," *Anesthesia and Analgesia Current Researches*, vol. 47, no. 6, pp. 717-&, 1968.

[2] N. Chauveau, "Resistor mesh model of a spherical head: Part 1: Applications to scalp potential interpolation," *Medical & Biological Engineering & Computing*, vol. 43, no. 6, pp. 694-702, Nov. 2005.

[3] Angiographic Head Phantoms, JZ Imaging & Consulting. Available: http://www.jzimaging.com/

[4] I.F. Triantis, "Tripolar-cuff deviation from ideal model : Assessment by bioelectric field simulations and saline-bath experiments," *Medical Engineering & Physics,* vol. 30, no. 5, pp.550-562, June 2008.

[5] M. R. Calabretta, "Mapping on the HEALPix grid," *Monthly Notices of the Royal Astronomical Society*, vol. 381, no. 2, pp. 865-872, Oct. 2007.

[6] K. M. Gorski, "HEALPix: A framework for high-resolution discretization and fast analysis of data distributed on the sphere," *Astrophysical Journal*, vol. 622, no. 2, pp. 759-771, Apr. 2005.

[7] B. F. Roukema, "A solution to the Isolatitude, Equi-area, Hierarchical Pixel-Coordinate System," arXiv:astro-ph/0409533v2, Sept. 2004.

[8] S. Gabriel, "The dielectric properties of biological tissues: II. Measurements in the frequency range 10 Hz to 20 GHz," *Phys. Med. Biol.,* vol. 41, pp. 2251-2269, 1996.

[9] F. W. Grover, *Inductance Calculations*. Dover Publications, New York, 1952.

[10] L.A. Geddes, "Measurement of the Direct-Current (Faradic) resistance of the electrode-electrolyte interface for commonly used electrode materials," *Annals of Biomedical Engineering*, vol. 29, no. 2, pp. 181-186, Feb. 2001.

[11] T. Oostendorp, "The Conductivity of the Human Skull: Results of *In Vivo* and *In Vitro* Measurements," *IEEE Transactions On Biomedical Engineering*, vol. 47, no. 11, pp. 1487-1492, Dec. 2000

[12] S. Goncalves, "*In Vivo* Measurement of the Brain and Skull Resistivities Using an EIT-Based Method and Realistic Models for the Head," *IEEE Transactions On Biomedical Engineering*, vol. 50, no. 6, pp. 754-767, Jun. 2003